Lattice Boltzmann simulations of attenuation-driven acoustic streaming

2003 J. Phys. A: Math. Gen. 36 5683

(http://iopscience.iop.org/0305-4470/36/20/322)

INSTITUTE OF PHYSICS PUBLISHING JOURNAL OF PHYSICS A: MATHEMATICAL AND GENERAL

J. Phys. A: Math. Gen. **36** (2003) 5683–5694 PII: S0305-4470(03)58230-0

Lattice Boltzmann simulations of attenuation-driven acoustic streaming

David Haydock[1,2] **and J M Yeomans**[2]

[1] Unilever R&D Colworth, Sharnbrook, Bedford MK44 1LQ, UK
[2] Department of Physics, Theoretical Physics, University of Oxford, 1 Keble Road, Oxford OX1 3NP, UK

Received 13 January 2003
Published 7 May 2003
Online at stacks.iop.org/JPhysA/36/5683

Abstract

We show that lattice Boltzmann simulations can be used to model the attenuation-driven acoustic streaming produced by a travelling wave. Comparisons are made to analytical results and to the streaming pattern produced by an imposed body force approximating the Reynolds stresses. We predict the streaming patterns around a porous material in an attenuating acoustic field.

PACS numbers: 43.25.Nm, 43.35.+d, 62.60.+v, 05.50.+q

1. Introduction

Acoustic streaming describes a steady flow field superimposed upon the oscillatory motion of a sound wave propagating in a fluid. It is a non-linear effect which occurs due to the presence of boundaries or because of damping of the wave [1, 2].

Acoustic streaming velocities are normally small compared to the velocity of the oscillatory fluid motion ($<\sim 10\%$). However, there are reports that it can enhance rate-limited processes such as diffusion [3, 4], heat transfer [1], the rate of sonochemical reactions [5] and mixing [6]. It can also have important and possibly undesirable effects in the study of acoustic levitation and the operation of theomoacoustic systems [7, 8]. The reasons behind this behaviour are unclear, and to understand and control the effects, it is important to better characterize the flow fields produced by acoustic streaming. For a few simple systems streaming velocities have been determined analytically. However, for more complex systems, analytical solutions will prove too difficult, so modelling methodologies need to be found. The aim of this paper is to describe one such approach, a lattice Boltzmann simulation, which can predict the acoustic streaming patterns from a direct solution of the Navier–Stokes equations.

There are two basic types of acoustic streaming. The first, Rayleigh streaming, is caused by relative oscillatory motion between the fluid and a boundary. The steady flow results from the rapid changes in the wave amplitude in the acoustic boundary layer. The effects

of attenuation on the primary wave, though present, are usually considered to be negligible. The second, Eckart streaming or quartz wind, results from the attenuation of the wave in the bulk fluid. Any boundary effects are neglected. Here momentum transfer from the wave is converted into a steady flow moving away from the source. Eckart streaming is often seen with quartz transducer systems such as ultrasonic probes.

Acoustic streaming was first considered analytically by Rayleigh in 1884 [9]. He predicted the streaming pattern for a standing wave between two parallel plates. More recently, Nyborg [1] corrected this solution and presented results for streaming caused by a travelling wave between two plates and for streaming around an infinitely long cylinder. Both of these studies were restricted to the case where the amplitude of the acoustic wave is very small. In 1978, Lighthill [2] published a further review of acoustic streaming in which he pointed out the necessity of including additional terms in the streaming equations for a more intense acoustic field. This included an approximate solution for higher amplitude turbulent streaming due to bulk attenuation, which he termed Stuart streaming.

To date there have been a small number of studies modelling acoustic streaming. Nightingale *et al* [10] used a standard computational fluid dynamics package to predict flow in breast cysts caused by Eckart streaming. The authors used the analogy between streaming and slow viscous flow to model the streaming as a flow produced by a body force which was calculated from the time-dependent first-order wave. This requires the wave profile to be known throughout the area of interest and assumes that there is no difference between the Lagrangian and Eulerian streaming velocities. Loh *et al* [11] used an incompressible computational fluid dynamics model to simulate streaming produced by ultrasonic flexural vibrations. This modelled acoustic streaming by producing the rotational incompressible boundary solution responsible for creating streaming [1] through oscillatory boundary conditions. However, as the simulation was truly incompressible no sound wave was present.

Stansell and Greated [12] used a lattice gas approach to model the acoustic streaming produced by a standing wave between two parallel plates. This is a simulation of the full Navier–Stokes equations of motion, and the acoustic streaming appears as a small correction to the oscillatory flow field. However, lattice gas simulations are inherently very noisy, and streaming could only be seen for high amplitudes and viscosities.

Recently Haydock and Yeomans [13] used a lattice Boltzmann algorithm to model acoustic streaming produced by the interaction of an acoustic wave with a boundary. Like the lattice gas approach, this is a simulation of the full Navier–Stokes equations, but it does not suffer from the same problems of noise. Here we demonstrate that lattice Boltzmann simulations can also be used to predict the velocity profiles due to the Eckart streaming produced by an attenuating wave. Hence, the lattice Boltzmann approach provides a method to obtain streaming patterns for complicated systems, where analytical investigations are not possible, and where boundary-driven and attenuation-driven streaming can coexist.

The next section of the paper introduces the lattice Boltzmann approach. In section 3, we compare the simulation results for attenuation-driven streaming in a pipe to the Nybourg solution and to streaming imposed by an imposed body force. Section 4 shows how it is possible to model acoustic streaming velocity profiles in the presence of a complex porous object.

2. The lattice Boltzmann algorithm

The lattice Boltzmann model we use is the single-relaxation-time Bhatnagar–Gross–Krook (BGK) scheme on a two-dimensional square lattice [14]. Lattice vectors are

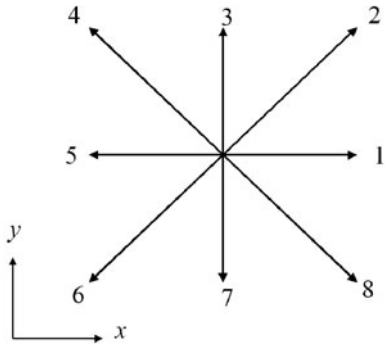

Figure 1. Numbering of lattice vectors in the lattice Boltzmann model.

$$\mathbf{e}_i = \left(\cos\left\{\tfrac{1}{4}\pi(i-1)\right\}, \sin\left\{\tfrac{1}{4}\pi(i-1)\right\}\right) \qquad i = 1, 3, 5, 7$$

$$\mathbf{e}_i = \left(\sqrt{2}\cos\left\{\tfrac{1}{4}\pi(i-1)\right\}, \sqrt{2}\sin\left\{\tfrac{1}{4}\pi(i-1)\right\}\right) \qquad i = 2, 4, 6, 8$$

together with a zero velocity vector $\mathbf{e}_0 = (0, 0)$ as shown in figure 1. A set of partial densities, $f_i(\mathbf{x}, t)$ associated with each lattice direction i are defined on each lattice site $\mathbf{x}$. These are related to the physical variables, density $\rho(\mathbf{x}, t)$ and velocity $\mathbf{u}(\mathbf{x}, t)$ by

$$\sum_i f_i(\mathbf{x}, t) = \rho(\mathbf{x}, t) \qquad \sum_i f_i(\mathbf{x}, t)\mathbf{e}_i = \rho(\mathbf{x}, t)\mathbf{u}(\mathbf{x}, t). \tag{1}$$

The partial densities evolve with time t according to

$$f_i(\mathbf{x} + \mathbf{e}_i, t + 1) - f_i(\mathbf{x}, t) = \frac{1}{\tau}\left(f_i - f_i^0\right) \tag{2}$$

where the local equilibrium distributions are

$$f_i^0 = \rho w_i\left\{1 + 3\mathbf{e}_i \cdot \mathbf{u} + \tfrac{9}{2}(\mathbf{e}_i \cdot \mathbf{u})^2 - \tfrac{3}{2}u^2\right\} \qquad i = 1, 2, \ldots, 8 \tag{3}$$

with $w_1 = w_3 = w_5 = w_7 = 1/9$ and $w_2 = w_4 = w_6 = w_8 = 1/36$ and

$$f_0^0 = \rho\left\{\tfrac{4}{9} - \tfrac{2}{3}u^2\right\}. \tag{4}$$

In equation (2), the left-hand side corresponds to the propagation step, where momentum is transferred, and the right-hand side represents the relaxation process which determines the viscous properties of the fluid. In the continuum limit, a Chapman–Enskog expansion of the numerical scheme reproduces the Navier–Stokes equations [14]

$$\partial_t \rho + \partial_\alpha \rho u_\alpha = 0 \tag{5}$$

$$\partial_t \rho u_\beta + u_\beta \partial_\alpha \rho u_\alpha + \rho u_\alpha \partial_\alpha u_\beta = -\partial_\beta P + \rho\nu\partial_\alpha[\partial_\beta u_\alpha + \partial_\alpha u_\beta] \tag{6}$$

with pressure $P = \rho/3$, kinematic viscosity $\nu = (2\tau - 1)/6$ and speed of sound $c_0 = 1/\sqrt{3}$.

3. Results for attenuation-driven streaming in a pipe

3.1. One-dimensional waves

Consider a two-dimensional container $0 \leqslant x \leqslant L_x, 0 \leqslant y \leqslant L_y$, where the walls have the same acoustic properties as the fluid. A plane acoustic wave of wavevector $k = 2\pi/\lambda$ and

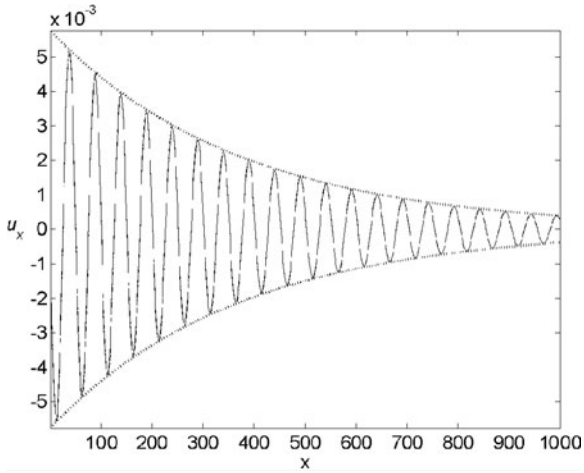

Figure 2. Comparison of velocity variation for one-dimensional simulation with theory when there is no time average velocity. Solid line: simulation, dashed line: theory, dotted line: theoretical amplitude as the wave attenuates with distance.

frequency ω propagates in the positive x-direction. The wave propagates from a source at $x = 0$ which produces a sinusoidal wave of velocity amplitude u_x.

We first consider a system that is translationally invariant in the y-direction. For this geometry no time-averaged flow is possible because there is no return path for the fluid. Instead a pressure gradient builds up. This geometry allows us to check that the primary sound wave in the simulation is behaving in the expected way.

For sufficiently large L_x that reflections from the end of the container can be ignored, the theoretical velocity amplitude of the wave is

$$u_{1x}(x, t) = U\,\mathrm{e}^{-\alpha x}\sin(wt - kx) \tag{7}$$

where α is the attenuation coefficient per unit length. This leads to Reynolds stresses and a resultant pressure gradient [1]

$$\partial_x P_2 = F_x = -\rho_0\langle 2u_{1x}\partial_x u_{1x}\rangle = \rho_0\alpha U^2\,\mathrm{e}^{-2\alpha x} \tag{8}$$

where $\langle\cdots\rangle$ denotes a time average.

To reproduce these results numerically using a lattice Boltzmann scheme, we chose a relaxation time $\tau = 0.8$ ($\nu = 0.1$), wavelength $\lambda = 50$ and an unperturbed density $\rho_0 = 1$. These give an attenuation coefficient $\alpha = 2.71 \times 10^{-3}$. A simulation length $L_x = 5000$ allowed significant attenuation of the beam and thus reduced reflections and $L_y = 3$ (for programming convenience). Periodic boundary conditions were used at $y = 0$ and $y = L_y$ and no-slip conditions, produced by a standard bounce-back scheme, at $x = 0$ and $x = L_x$ [15].

The sound wave was generated by adding a sinusoidal pressure and momentum variation

$$f_i^+ = f_i + \delta\rho 3 w_i e_i \sin(\omega t) \qquad i = 1, 2, 8 \tag{9}$$

at $x = 0$ for all y. To reduce reflections an absorbing boundary condition

$$f_i^+ = f_i - \delta\rho 3 w_i e_i\,\mathrm{e}^{-\alpha x}\sin(\omega t - kx) \qquad i = 4, 5, 6 \tag{10}$$

was added at $x = L_x$ for all y. This gives a sound wave with density amplitude $\delta\rho = 0.01$ and velocity amplitude $U = \delta\rho c = 0.0058$ at $x = 0$.

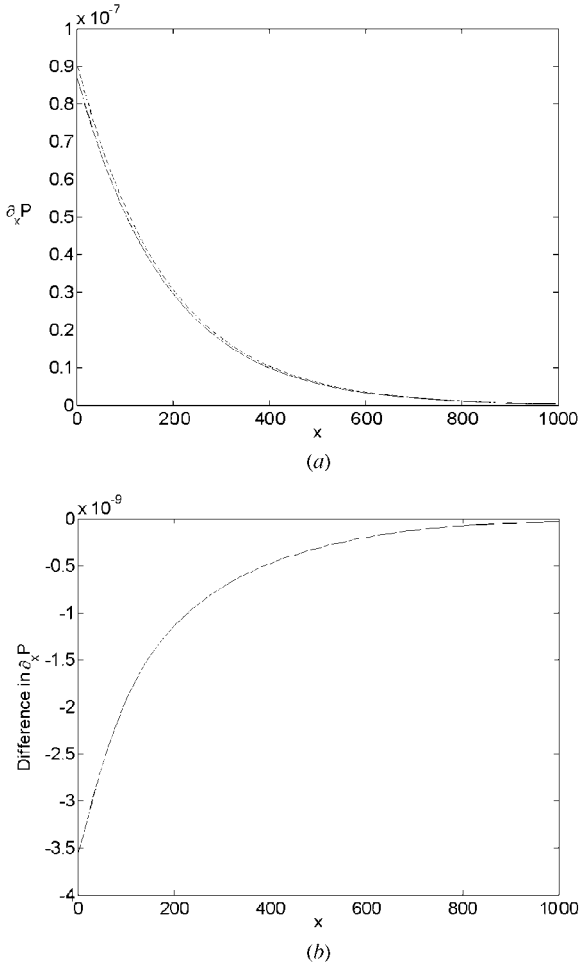

Figure 3. (*a*) Second-order pressure gradient for a one-dimensional simulation with no time average velocity. Solid line: simulation, dashed line: theory. (*b*) Difference in between the lattice Boltzmann simulation and theory for the second-order pressure gradient.

Figure 2 shows the velocity variation in the wave as a function of x, the distance from the source. The simulation waveform cannot be distinguished from the theoretical linear waveform. This demonstrates that there are no significant reflections from $x = L_x$, and that the wave is not developing significant time dependent non-linearities. Figures 3(*a*) and (*b*) show the second-order pressure gradient $\partial_x P_2$ and the difference between the theoretical prediction and the simulation, respectively. Again there is good agreement with the theory.

3.2. Streaming in a channel

When the sound field does not completely fill the channel recirculatory flow is possible. This allows the force due to the Reynolds stresses to produce a time-averaged steady flow known as Eckart streaming. We simulate this geometry and compare our results to an analytic solution due to Nyborg [1] and to the streaming obtained by imposing an appropriate body force.

Nyborg [1] considered a channel where the first-order velocity is given by (7) for $0 \leqslant y \leqslant l_s$, where $2l_s$ is the dimension of the sound source and is zero for $l_s < y \leqslant L_y$. He found a streaming velocity

$$u_2 = \frac{\alpha U^2}{2\nu}\left\{\left(2L_y y - y^2 - l_s^2\right) + [2 - 3(l_s/L_y)^2 + (l_s/L_y)^3]y(y - L_y)/2\right\}. \tag{11}$$

The solution assumes a perfectly collimated beam, no reflections and weak attenuation of the wave. It also assumes a low intensity beam so that no higher harmonics are produced in the wave and small gradients in the streaming velocity, so the equation

$$\mu\partial_x^2 u_{2x} - \partial_x P_2 = -F_x = 2\rho_0\langle u_{1x}\partial_x u_{1x}\rangle \tag{12}$$

can be used. This is a difficult limit to achieve numerically because weak attenuation implies unwanted reflections at $x = L_x$ or a simulation prohibitively expensive in computational resources. Therefore, we also compare our simulation to one in which streaming is produced using an imposed 'body force' due to the Reynolds stresses [1, 10]

$$F_x = \rho_0\alpha U^2 \tag{13}$$

as in Nightingale *et al* [10].

The parameters used in the lattice Boltzmann simulation were $\tau = 0.8, \lambda = 50$ and $\rho_0 = 1$ as in section 3.1. The size of the simulation domain was $L_x = 2000$, $L_y = 400$. No-slip boundary conditions were applied at $x = 0$, $x = L_x$ and $y = L_y$. Slip boundary conditions at $y = 0$ allowed us to exploit reflectional symmetry and simulate a system $-L_y \leqslant y \leqslant L_y$. A sound wave was generated at the centre of the system by applying the sinusoidal variation (9) for $x = 0$, $0 \leqslant y \leqslant l_s$. Absorbing boundary conditions (10) were applied at $x = L_x$, $0 \leqslant y \leqslant l_s$. We took $l_s = 200$ to provide a sufficient length relative to the wavelength to produce a collimated field. To determine the streaming velocities, we allowed 3000 wave cycles for the simulation to reach a steady state, then took the time average over 50 cycles. This gave a run time of 31 h on a P4 2.5 GHz PC with 1 GB 800 MHz RDRAM.

Figure 4(*a*) shows the behaviour of the sound wave within the simulation box. Figure 4(*b*) is a one-dimensional cross section at $y = 100$ comparing details of the waveform with the primary wave used in the Nyborg theory. They show that the simulation wave is reasonably well collimated but some energy is transferred from the primary wave into the y-direction producing waves that are reflected from the boundary at $y = L_y$. Note that the simulation produces a more physical transition from the collimated sound field to the surrounding fluid than the theory.

Figure 5(*a*) shows the vector plot for the streaming velocity. Figure 5(*b*) compares the streaming velocity u_{2x} at $x = 250$ (the maximum of u_{2x}) to that produced using the body force predicted by (13) over all x, $y < l_s$. There is good agreement between the full streaming simulation and the simulation using the body force. The differences occur at the edge of the beam where the body force imposes a perfectly collimated wave.

Figure 5(*c*) shows the velocity profile predicted for u_{2x} by the analytical result (11). There is an order of magnitude difference between the theoretical prediction and the two simulations. We assumed that this is because the theory holds in the limit of zero attenuation, a limit that is not accessible numerically. To check that it was possible to approach the theoretical limit, we examined the effects of reducing the attenuation by running a simulation with $L_x = 10\,000$, $L_y = 400$ and $\tau = 0.55$. We used 5000 time steps for the simulation to reach a steady state and took the time average over 50 cycles. This gave a maximum streaming velocity $u_2x \sim 2\times10^{-3}$ which is approximately half that predicted by Nyborg. Thus a reduction in the attenuation does indeed lead to results that approach the Nyborg solution. However, the simulation took 59 h using 16 nodes of a IBM 1 GHz Linux cluster and any closer match to the Nyborg limit would

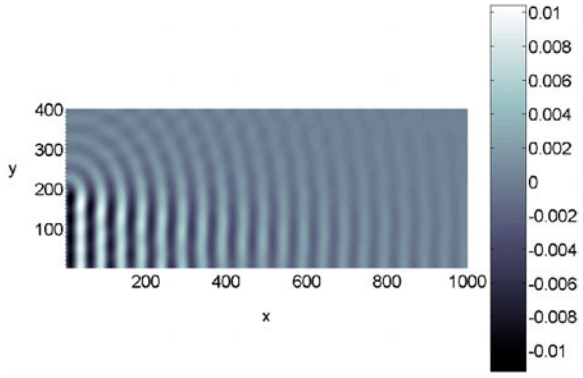

(*a*)

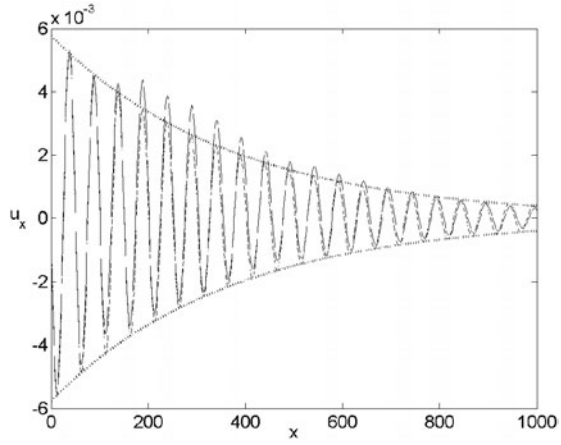

(*b*)

Figure 4. (*a*) Density amplitude of the sound wave after 5050 cycles for the $L_x = 2000$, $L_y = 400$, $\lambda = 50$, $\tau = 0.55$ and $l_s = 200$ simulation. For clarity only the first 1000 lattice points are shown in the propagation direction. (Slip boundaries at $y = 0$ mean that this forms a plane of reflectional symmetry.) (*b*) Comparison of the velocity variation at $y = 100$ for the $L_x = 2000$, $L_y = 400$, $\lambda = 50$ and $\tau = 0.55$ simulation after 5050 cycles with the theoretical wave. Solid line: simulation, dashed lines: theory (7), dotted line: theoretical amplitude as the wave attenuates with distance. Differences are due to reflections at L_y.

be computationally too expensive. In addition, as the viscosity is reduced, non-linearities which are not included in the theory but are present in the simulation will become more important.

To relate the non-dimensional lattice Boltzmann parameters u, x, t, ν, α and F to real world parameters u', x', t', ν', D' and F', we use a characteristic velocity V and length L of the real system as follows: $u' = Vu, x' = Lx, t' = (L/V)t, \nu' = VL\nu, \alpha' = L^{-1}\alpha$, $F'(\rho V^2/L)F$ and $V = c_0'/c_0$. If we consider a wave propagating in air assuming international standard atmosphere properties at sea level [16] ($c_0' = 340\ \mathrm{m\,s^{-1}}$, $\rho_0' = 1.2\ \mathrm{kg\,m^{-3}}$, $\nu' = 1.4 \times 10^{-5}$) and choosing $\nu = 0.0333$ then $V = 588.9\ \mathrm{m\,s^{-1}}$, and $L = 2.377 \times 10^{-7}$. The simulation used to model streaming in a channel has real parameters $f' = 28.6$ MHz, $L_x' = 475\ \mu$m, the half space $L_y' = 95$ mm, the intensity of the wave $I = 2.36\ \mathrm{kW\,m^{-2}}$, where $I = 0.5\rho_0 c_0 U^2$ [2], and each time step represents 0.4 ns.

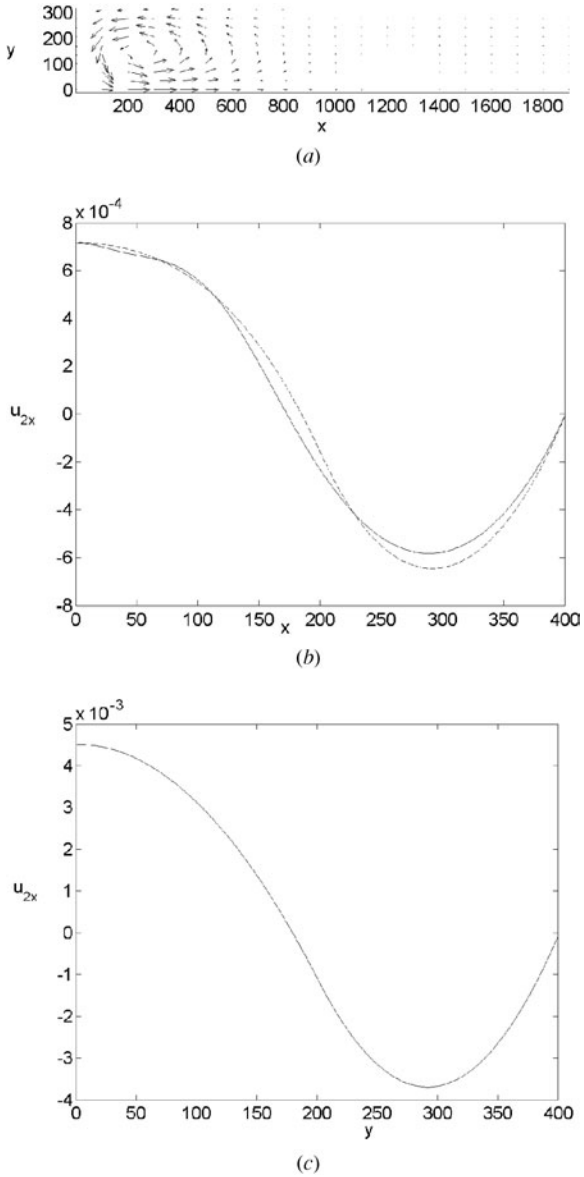

Figure 5. (*a*) Vector plot of the streaming velocity for the $L_x = 2000$, $L_y = 400$, $\lambda = 50$ and $\tau = 0.55$ simulation. (*b*) Streaming velocity at $x = 250$ for the $L_x = 2000$, $L_y = 400$, $\lambda = 50$, $\tau = 0.55$ simulation. Solid line: full streaming simulation, dotted line: streaming simulated by using a body force. (*c*) Streaming velocity for parameters $L_x = 2000$, $L_y = 400$, $\lambda = 50$, $\alpha = 0.0027$ ($\tau = 0.55$) from the theory presented by Nyborg [1].

4. Streaming around and through a porous material

We have shown that lattice Boltzmann simulations can be used to model attenuation-driven acoustic streaming and, in a previous paper [13], we showed that these simulations can also model streaming produced by the interaction with boundaries. Therefore, we can hope to

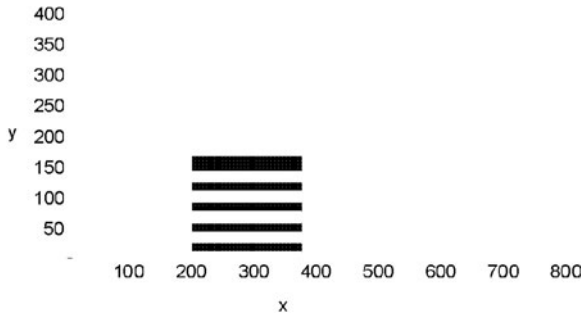

Figure 6. Porous material geometry.

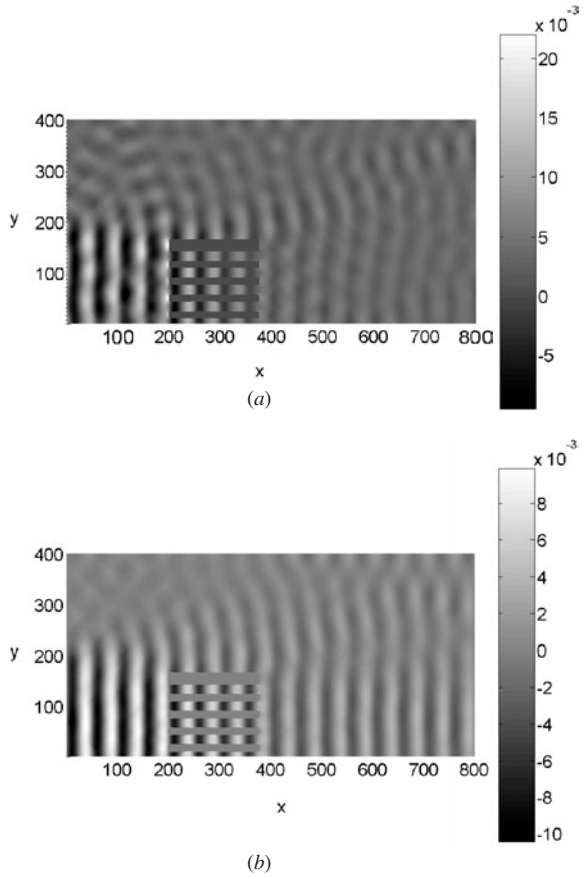

Figure 7. (*a*) Density field from the simulation of streaming around the porous material. Slip boundaries at $y = 0$ mean that this forms a plane of reflectional symmetry. (*b*) x velocity field from the simulation of streaming around a porous material. Slip boundaries at $y = 0$ mean that this forms a plane of reflectional symmetry.

predict the streaming patterns associated with objects placed in the acoustic field as long as there is a large difference in acoustic impedance between the object and the fluid so that the

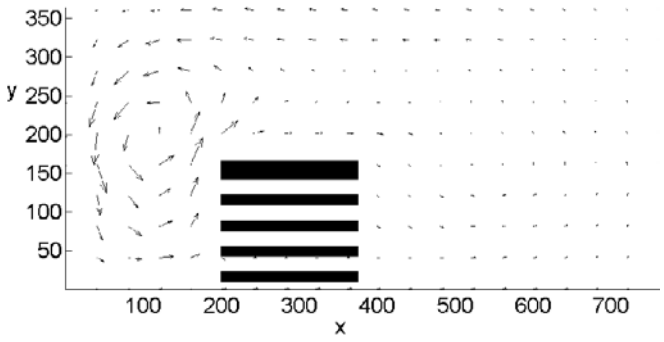

Figure 8. Vector plot of the streaming field around the porous material.

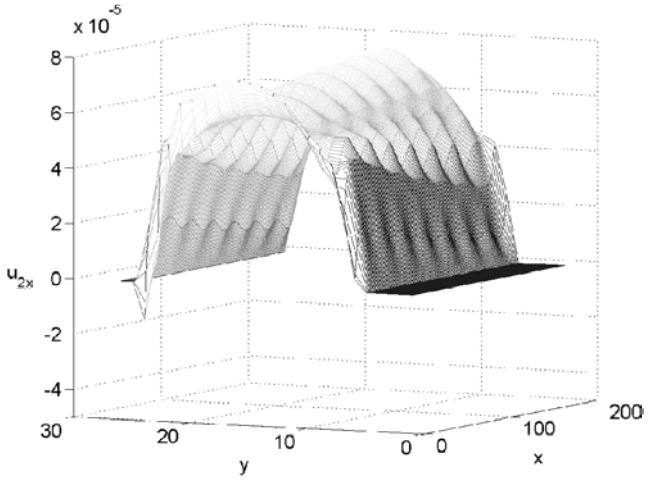

(*a*)

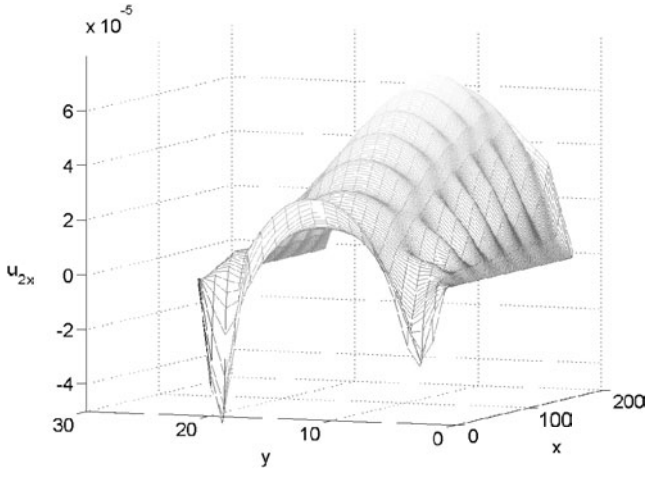

(*b*)

Figure 9. (*a*) *x* component of Lagrangian streaming velocity through one of the channels of the porous solid. (*b*) *x* component of Eularian streaming velocity through one of the channels of the porous solid.

boundary conditions may be modelled as no-slip. This is typical of many solids placed in a vibrating fluid such as water or air.

As an example we consider a porous material consisting of nine parallel channels shown in figure 6. (Again we display only the part of the simulation for $y > 0$: slip boundaries at $y = 0$ mean that this forms a plane of reflection symmetry.) Here $L_x = 800$, $L_y = 400$, $\lambda = 50$, $\tau = 0.6$ ($\nu = 0.033$) and $l_s = 200$, and the solid dimensions are $199.5 \leqslant x < 375.5$, $l_y = 333/2$, the channel widths $l_c = 20$, with a pitch of 33. The initialization time was 1000 cycles and the streaming velocities were evaluated over the following 50 cycles.

Figure 7(a) shows the first-order density variation of the sound wave after 1050 cycles. Figure 7(b) shows the first-order velocity field u_{1x} after 1050 cycles. Figure 8 shows the vector plot of the second-order streaming field after the simulation has reached equilibrium. As expected both the acoustic field and the streaming velocities are relatively complex. The presence of the material produces large reflections setting up a 'standing wave' at $0 < x < 199.5$. This does not produce the classic streaming patterns associated with a standing wave due to the lack of appropriate boundaries but rather produces Eckart streaming due to the attenuation. The Reynolds stresses associated with this attenuation produce two time-averaged vortices which form at each side of the material and join just above the material.

Within the channels there is a lower amplitude wave as some proportion of the wave is transmitted through the material. As expected within the pores a Poiseuille flow is produced. This is due to bulk attenuation and attenuation due to the material boundaries, which will both contribute to acoustic streaming. Figure 9(a) shows the second-order Lagrangian streaming velocity (time averaging the momentum), and figure 9(b) is the second-order Eularian streaming velocity (averaging velocity only). Note that there is a significant difference between the two methods of determining velocity. A simple time average of the velocity (figure 9(b)) produces a flow that clearly does not conserve mass where the Lagrangian evaluation does conserve mass except for the inclusion of a small quantity of noise at second order.

5. Conclusions

In this paper we have shown that lattice Boltzmann simulations can be used to model attenuation-driven acoustic streaming. The lattice Boltzmann approach solves the full Navier–Stokes equations, so once boundary conditions are implemented that produce and correctly constrain the wave, streaming is automatically generated. Thus the method is free from the constraint of needing to determine the harmonic solution as a boundary condition for the model.

We have also demonstrated that the lattice Boltzmann approach can be used to determine the streaming patterns produced around a complex object placed in the acoustic field where the object itself has a significant effect on the harmonic wave and hence the streaming produced. Here, there can be a significant difference between the two methods of evaluating the time-averaged velocity at a point and the time average mass flow.

These simulations will prove useful in understanding the acoustic enhancement of rate limiting processes such as diffusion, heat transfer, sonochemical reactions or mixing. They will also have application in predicting the flow in ultrasonically driven microfluidic devices.

References

[1] Nyborg W L M 1965 Acoustic streaming *Physical Acoustics* vol 2B ed W P Mason and R N Thurston (New York: Academic) pp 265–331

[2] Lighthill J 1978 Acoustic streaming *J. Sound Vib.* **61** 391–418
[3] Arkhangel'skii M E and Statnikov Y G Diffusion in heterogeneous systems *Physical Principles of Ultrasonic Technology* vol 2 ed L D Rozendurg (New York: Plenum)
[4] Floros J and Liang H 1994 Acoustically assisted diffusion through membranes and biomaterials *Food Technology* **48** 79–84
[5] Booth J, Compton R G, Hill E, Marken F and Rebbitt T O 1997 A novel approach for the quantitative kinetic study of reactions at solid/liquid interfaces in the presence of ultrasound *Ultrason. Sonochem.* **4** 1–7
[6] Suri C, Takenaka K, Kojima Y and Koyama K 2002 Experimental study of a new liquid mixing method using acoustic streaming *J. Chem. Engng. Japan* **35** 497–502
[7] Yarin A L, Brenn G, Kastner O, Rensink D and Tropea C 1999 Evaporation of acoustically levitated droplets *J. Fluid Mech.* **399** 151–204
[8] Backhaus S and Swift G W 2000 A thermoacoustic-Stirling heat engine: detailed study *J. Acoust. Soc. Am.* **107** 3148–66
[9] Rayleigh L 1929 *The Theory of Sound* (London: Macmillan)
[10] Nightingale K R, Kornguth P J and Trahey G E 1996 Streaming detection: improvements in sensitivity *IEEE Ultrasonics Symposium Proceedings* pp 1261–4
[11] Loh B G, Hyum S, Ro P I and Kleinstreuer C 2002 Acoustic streaming induced by ultrasonic flexural vibrations and associated enhancement of convective heat transfer *J. Acoust. Soc. Am.* **111** 875–83
[12] Stansell P and Greated C A 1997 Lattice gas automation simulation of acoustic streaming in a two-dimensional pipe *Phys. Fluids* **9** 3288–99
[13] Haydock D and Yeomans J M 2001 Lattice Boltzmann simulations of acoustic streaming *J. Phys. A: Math. Gen.* **34** 5201–13
[14] Chen S and Doolen G D 1998 Lattice Boltzmann method for fluid flows *Annu. Rev. Fluid Mech.* **30** 329–64
[15] Rothman D H and Zaleski S 1997 *Lattice Gas Cellular Automata: Simple Models of Complex Hydrodynamics* (Cambridge, UK: Cambridge University Press)
[16] Rogers G F C and Mayhew Y R 1985 *Thermodynamic and Transport Properties of Fluids* 3rd edn. (Oxford, UK: Basil Blackwell)